

## Aluminum Acceptor Ionization Energies in 4H-SiC for Low Dose, Ultra-High Energy (> 1MeV) Implants

Collin Hitchcock<sup>1,a\*</sup>, Reza Ghandi<sup>1,b</sup>, Peter Deeb<sup>1,c</sup>, Stacey Kennerly<sup>1,d</sup>,  
Mohamed Torky<sup>2,e</sup>, T. Paul Chow<sup>2,f</sup>

<sup>1</sup>GE Research, 1 Research Circle, Niskayuna, NY 12309, USA

<sup>2</sup>Rensselaer Polytechnic Institute, 110 8th Street, Troy, NY 12180, USA

<sup>a</sup>Collin.Hitchcock@ge.com, <sup>b</sup>Ghandi@ge.com, <sup>c</sup>Peter.Deeb@ge.com, <sup>d</sup>Stacey.Kennerly@ge.com,  
<sup>e</sup>torkym@rpi.edu, <sup>f</sup>chowt@rpi.edu

**Keywords:** Superjunction Diode, Temperature Dependent Hall Effect, Capacitance-Voltage, Incomplete Ionization, Aluminum Activation, Aluminum Acceptor Ionization Energy

**Abstract** MeV level aluminum implants into 4H-SiC were performed as part of superjunction diode fabrication. Measurement of resistance test structures produced resistivities well above expected values with large decreases at elevated temperatures. Capacitance-voltage measurements indicate a high activation rate of the implanted aluminum. Temperature dependent Hall measurements produce reasonable hole mobilities with acceptor ionization energies of approximately 330meV, well above the 200meV expected for low concentration aluminum doping in 4H-SiC.

### Introduction

Aluminum is a deep acceptor in 4H silicon carbide with a generally accepted ionization energy of approximately 200meV for low doping concentrations. The ionization energy is known to decrease with increasing dopant concentration to below 100meV at concentrations near the solubility limit [1,2]. There are indications that, at low acceptor concentrations, the ionization energy exceeds the 200meV generally accepted value [3-7]. Here, we study MeV-level, ultra-high energy (UHE) aluminum implants utilized for p-pillar formation in superjunction (SJ) devices.

### Experimental Samples

Starting with n-type,  $1 \times 10^{15} \text{cm}^{-3}$ , 12 $\mu\text{m}$  thick epitaxial layers grown on n+ 4H-SiC substrates, SJ p-pillars and n-pillars were fabricated using masked UHE implants of aluminum and nitrogen respectively. Multiple implants with varying energies were performed targeting a net uniform  $1 \times 10^{16} \text{cm}^{-3}$  doping concentration throughout the entire 12 $\mu\text{m}$  deep epitaxial region [8]. After additional lower energy p-type implantations to form diode anodes and edge termination structures, dopants were activated at anneal conditions ranging from 1700 to 2000°C. Subsequent processing resulted in vertical p-n SJ diodes. Details of the diode fabrication and performance can be found elsewhere in these proceedings [9].

In addition to the diodes, a number of test structures were co-fabricated on-wafer in order to validate the fabrication processes and to delineate the specifics of device performance. Transmission-line structures (TLMs) and Van der Pauw structures (VDPs) allowed for contact and sheet resistance measurements of implanted layers. Along with purpose-fabricated Hall bars, the VDPs were also used for Hall effect measurements to determine the free carrier concentration and mobility. Finally, a number of diode structures with large area, single-type pillar doping through the entire 12 $\mu\text{m}$  drift region were available in both n-type and p-type versions for electrical testing of the bulk implanted layers.

## Experimental Results

Resistivities extracted using the p-pillar TLMs and VDPs are shown in Table 1 as a function of activation anneal temperature and measurement temperature. Room temperature results are much higher than expected, with calculated free hole concentrations of between  $1.0 \times 10^{14} \text{cm}^{-3}$  and  $1.2 \times 10^{14} \text{cm}^{-3}$  (assuming  $100 \text{cm}^2 \text{V}^{-1} \text{s}^{-1}$   $25^\circ \text{C}$  hole mobility for this resistivity measurement only) and a corresponding active ionized acceptor ratio of only about 1% of the implanted dose. Also, as illustrated in Table 1, resistivity decreased by an order of magnitude as temperature increased from room temperature to  $200^\circ \text{C}$ , with free hole concentrations rising to between  $2.5 \times 10^{15} \text{cm}^{-3}$  and  $2.7 \times 10^{15} \text{cm}^{-3}$  (assuming  $50 \text{cm}^2 \text{V}^{-1} \text{s}^{-1}$   $200^\circ \text{C}$  hole mobility for this resistivity measurement only). There was no significant dependence of the measured resistivity on the activation anneal temperature. Since a 200meV Al acceptor ionization energy results in roughly 40% ionization at room temperature, an ionized acceptor increase of an order of magnitude with temperature should not be possible.

Table 1: Sheet resistances of p-pillar implanted regions

Activation Anneal	VDP $25^\circ \text{C}$ ( $\Omega$ )	TLM $25^\circ \text{C}$ ( $\Omega$ )	VDP $200^\circ \text{C}$ ( $\Omega$ )	TLM $200^\circ \text{C}$ ( $\Omega$ )
<b>1700°C, 30 min</b>	$4.2 \times 10^5$	$4.27 \times 10^5$	$3.8 \times 10^4$	$3.89 \times 10^4$
<b>1800°C, 120 min</b>	$4.5 \times 10^5$	$4.56 \times 10^5$	$3.7 \times 10^4$	$3.84 \times 10^4$
<b>1900°C, 60 min</b>	$4.7 \times 10^5$	$4.65 \times 10^5$	$3.7 \times 10^4$	$4.10 \times 10^4$
<b>2000°C, 40 min</b>	$5.0 \times 10^5$	$4.57 \times 10^5$	$3.7 \times 10^4$	$3.85 \times 10^4$

Fig. 1 illustrates the results of capacitance-voltage (CV) measurements taken on large area p-pillar implanted regions. Since the applied DC bias will field-ionize dopants that are incompletely ionized under equilibrium conditions, this technique will measure total activated implant doses. Fig. 1a shows the CV test structure schematically; as DC bias increases, the bottom portion of p-pillar region adjacent to the n-type substrate is probed. Raw CV curves are shown in Fig. 1b, and the differential  $1/C^2$  doping extraction shown in Fig. 1c indicates a near constant active dopant concentration very close to the  $1 \times 10^{16} \text{cm}^{-3}$  implanted dose throughout the probed region directly above the N+ substrate surface. Fig. 1d indicates that the probed region extends approximately  $2 \mu\text{m}$  into the p-pillar region from the substrate interface. Table 2 shows median differential  $1/C^2$  extracted dopings for all 4 activation anneal temperatures taken both at room-temperature and at  $200^\circ \text{C}$ ; detailed curves for the  $200^\circ \text{C}$  measurement temperature are qualitatively similar to those in Fig. 1. All extracted acceptor concentrations are close to the  $1 \times 10^{16} \text{cm}^{-3}$  implanted value. An example CV of a full SJ diode, implementing both n-pillar and p-pillars, is shown in Fig. 2. No appreciable unexpected differences between CV curves taken at AC frequencies between 1kHz and 1MHz were observed. The near full-implant level hole concentrations measured by CV independent of temperature and frequency further point to lower-than-expected ionization of the aluminum dopant.

Hall effect measurements were performed using two different systems. Low noise measurements were obtained measuring p-pillar VDPs between  $-50^\circ \text{C}$  and  $50^\circ \text{C}$  using a Lake Shore Hall effect system equipped with a cryogenic cold head and electromagnets capable of  $\pm 2 \text{kG}$ . Additionally, p-pillar Hall bars were measured on a second system at a fixed, reversible field of  $4.8 \text{kG}$  and employing a localized package heating system from room temperature up to  $200^\circ \text{C}$ . Measured carrier concentrations for all four activation anneal conditions are shown in Fig. 3 on an Arrhenius style plot along with theoretical curves fitted to experiment by adjusting unknown parameters; Hall mobilities are inset at the lower left. Hall scattering factor was assumed to be unity for all analyses. As with the resistance and CV measurements, there were no significant differences between experimental Hall measurement results for any of the experimental activation anneal temperatures. Theoretical Hall curves were generated in a spreadsheet by iterative numerical solution of the Fermi-Dirac occupancy of the valence band and acceptor states. Parameters for the theoretical

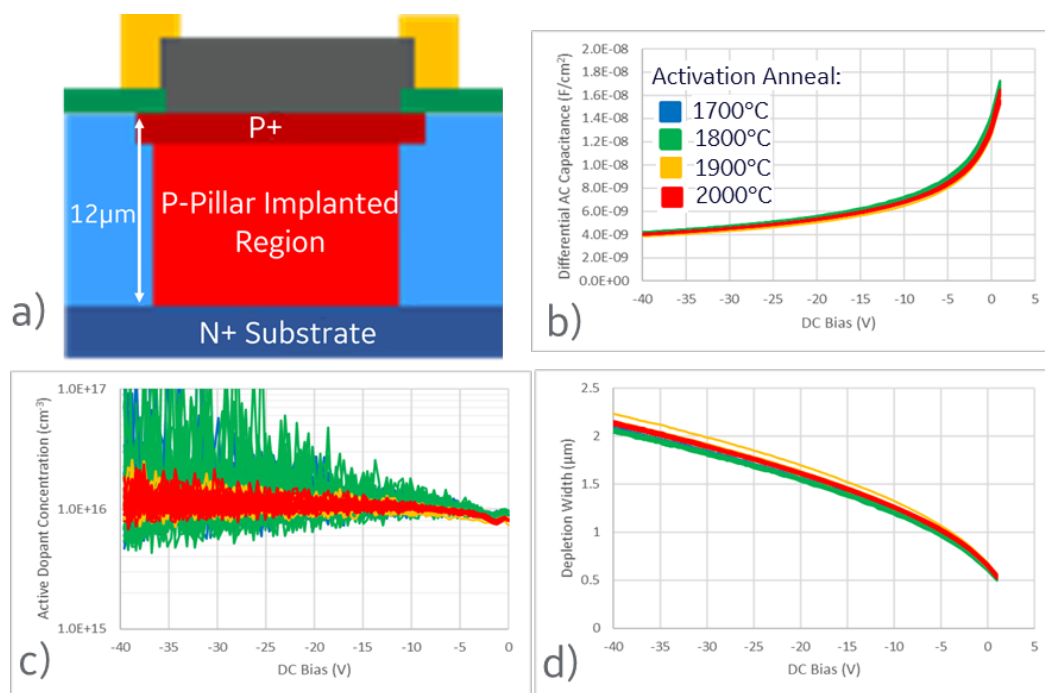


Fig. 1: Capacitance-Voltage Measurements (25°C, 25mV 100kHz AC signal) of p-pillar test structures (results for approximately 25 structures at each anneal temperature) (a) Schematic CV test structure, (b) Raw capacitance measurement, (c) Extracted doping as a function of bias voltage, (d) Extracted measurement location (depth into the p-type implanted region from the implant/substrate interface).

Table 2: CV Extracted Median Acceptor Concentrations for P-Pillar UHE Implanted Test Structures.

Anneal, Measured Temp	25°C (cm <sup>-3</sup> )	200°C (cm <sup>-3</sup> )
1700°C	$1.09 \times 10^{16}$	$1.06 \times 10^{16}$
1800°C	$1.12 \times 10^{16}$	$1.05 \times 10^{16}$
1900°C	$1.02 \times 10^{16}$	$1.02 \times 10^{16}$
2000°C	$1.04 \times 10^{16}$	$1.03 \times 10^{16}$

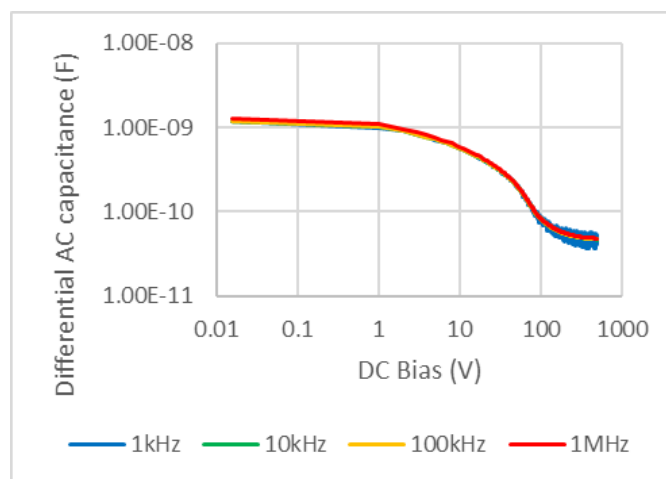


Fig. 2: 25mV CV measurements of 0.05cm<sup>2</sup> SJ diodes as a function of AC frequency.

curves are the total active acceptor concentration, the ionization energy of the acceptor level, and the ratio of compensation by n-type dopants and defects (which are assumed to be at a sufficient energy above the acceptor level to be 100% ionized). Additionally, P<sup>+</sup> structures (shown for reference) are well fit by a 70meV ionization energy curve, consistent with theory.

In the low temperature freeze-out region, where carrier concentration is independent of active acceptor concentration, the best fit to experiment is obtained with an acceptor energy of 330meV and a compensation ratio of 20%. Comparing experiment to theoretical curves with a compensation ratio of the minimum reasonable value of 10% (based on initial epitaxial doping) produces a reasonable fit assuming an acceptor energy of 350meV, and examining increased compensation ratios allows a fit at up to 60% compensation and 290meV before the slope of the experimental curve diverges significantly from the theory and the horizontal asymptote of the experimental curve in the high temperature region begins to converge above the implanted acceptor dose.

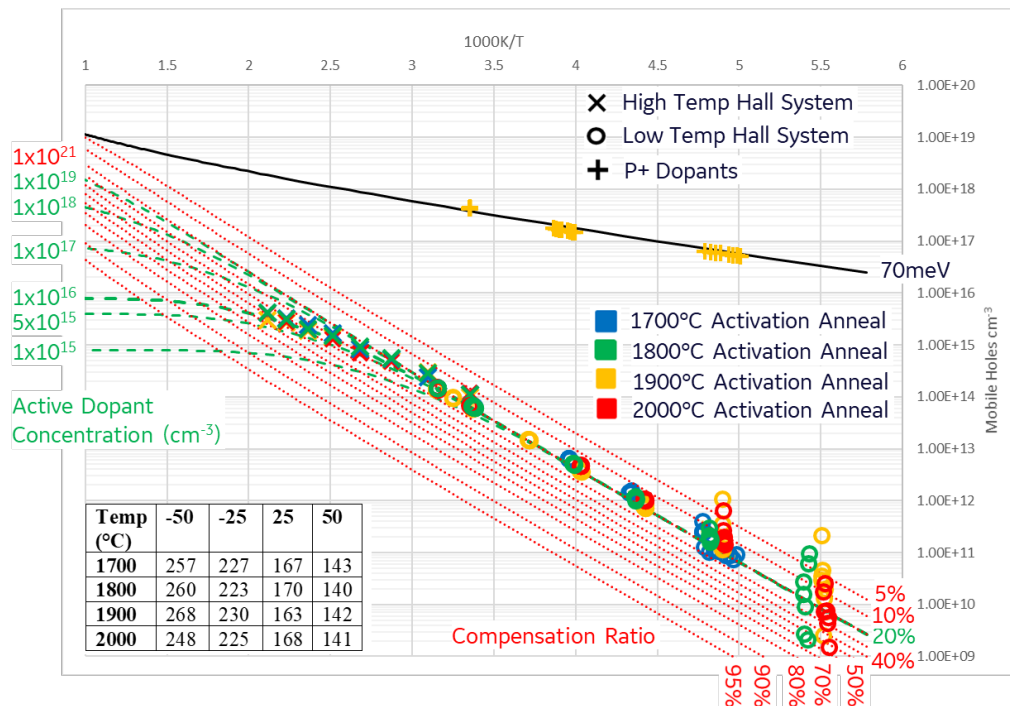


Fig. 3. Hall mobile hole concentration and 330meV ionization energy theoretical curves with varying active dopant doses and compensation ratios for UHE implanted p-pillar regions. Hall mobilities ( $\text{cm}^2\text{V}^{-1}\text{s}^{-1}$ ) as a function of anneal and measurement temperatures are inset at lower left.

## Conclusion

Based on CV-measured acceptor concentrations very close to the implanted dose (independent of frequency and temperature), we conclude that UHE implants of aluminum at the  $1 \times 10^{16} \text{cm}^{-3}$  level are close to 100% activated at all experimental activation anneal conditions. Based on the temperature dependent resistance structure measurements combined with the behavior of temperature-dependent Hall measurements, we conclude that these implants result in acceptor ionization energies significantly higher than accepted low-doping values, with values between 290meV and 350meV. Since similar recent results in the literature report good high temperature Hall fits of moderate Al implanted layers with 100% activation by assuming partial activation into an additional, high ionization energy acceptor level [7], we postulate that low dose implanted Al is activated at least partially on an alternate SiC lattice site resulting in a higher effective acceptor ionization energy.

### Acknowledgement

The information, data, or work presented herein was funded in part by the Advanced Research Projects Agency-Energy (ARPA-E), U.S. Department of Energy, under Award Number DE-AR0001007. The views and opinions of authors expressed herein do not necessarily state or reflect those of the United States Government or any agency thereof.

### References

- [1] T. Kimoto and J. Cooper, Fundamentals of Silicon Carbide Technology, 1st ed, (Wiley & Sons Singapore, 2014), p. 21
- [2] C. Darmody and N. Goldsman, J. Appl. Phys. 126, 145701 (2019).
- [3] J. Weisse, M. Hauck, T. Sledziewski, M. Tschiesche, M. Krieger, A. Bauer, H. Mitlehner, L. Frey, and T. Erlbacher, Mat. Sci. Forum 924, 184 (2018).
- [4] T. Troffer, M. Schadt, T. Frank, H. Itoh, G. Pensl, J. Heindl, H. P. Strunk, and M. Maier, Phys. Stat. Sol. (a) 162, 277 (1997)
- [5] N. Saks, A. Agarwal, S-H. Ryu, and J. Palmour, J. App. Phys. 90, 2796 (2001)
- [6] H. Matsuura, Mat. Sci. Forum, 389-393, 679 (2002)
- [7] J. Weisse, M. Hauck, M. Krieger, A. Bauer, and T. Erlbacher, AIP Advances 9, 055308 (2019)
- [8] P. Thieberger, C. Carlson, D. Steski, R. Ghandi, A. Bolotnikov, D. Lilienfeld, and P. Losee, Nuclear Instruments and Methods in Physics Research Section B, 442, 36 (2019)
- [9] R. Ghandi, C. Hitchcock, and S. Kennerly, 13<sup>th</sup> ECSCRM (2021)